Studies on recuperation systems for fluorinated greenhouse gases at the LHC experiments

Hsuan-Chu Chen
CERN, Geneva, Switzerland

Abstract
The CERN EP-DT-FS Gas team identified several strategies to reduce greenhouse gas emissions from LHC particle detectors. On Compact Muon Solenoid detector, CERN has implemented R134a ($C_2H_2F_4$) recuperation system to recover R134a from the exhaust of Resistive Plate Chamber. This report focuses on the studies of SF_6 recovery using adsorption processes. Both experiments and simulations are done to test whether adsorption is a potential method for SF_6 recovery. The experiment shows that both z5 and z10 are promising materials for the separation via adsorption, while sometimes thermal regeneration is needed. The simulation on the other hand indicates that adsorption may be helpful at the second stage of SF_6 recovery.

1 Introduction

Around the Large Hadron Colliders (LHC) accelerator ring, there are four particle detectors - ATLAS, CMS, ALICE and LHCb. Depending on the purpose and the geometry of the gas detectors, different gas mixtures are required. For CMS, Resistance Plate Chamber (RPC) works with a gas mixture made of R134a/iC_4H_{10}/SF_6 in a ratio 95.2/4.5/0.3. The main problem related to the use of these fluorinated gases is their high global warming potential (GWP). Furthermore, their life span in the atmosphere can reach values as high as 3200 years [1]. In 2021-2022, the fluorinated gases accounted for about 78% of the Organization's direct emissions [2]. To reduce the Greenhouse Gases (GHGs) impact at CERN, different strategies are adopted.

The main strategy consists in recirculating the huge volume of the detector (in the order of m^3) in the gas system. However, it is not possible to work with 100% of recirculation. In fact, this causes the accumulation of air (due to leaks) and reactive polluting species. Therefore, most of the system work with a recirculation fraction of 90%, and the remaining 10% is exhausted to the atmosphere. In some cases, the gas is fed to recovery plants where the fluorinated components of the mixture are separated from the other components, stored and then re-injected in the mixer through a dedicated line. Currently, CERN has implemented four recovery systems, two on CMS and two on LHCb, recovering CF_4, R134a, and C_4F_{10}.

2 Aims and Objectives

Due to the new EU regulation on F-gases and its high GWP, the plan of SF_6 ($GWP_{100\,\text{years}} = 22800$) recuperation system has started.

Figure 1 schematizes the separation process of R134a from RPC mixture and SF_6 from the recovery exhaust. The concentration of SF_6 in the exhaust of R134a recovery system is very low (1.3%), so it is impossible to obtain pure SF_6 using volatility difference only. Therefore, the goal of this project is to understand if the methodology can be applied to separate SF_6 either directly from the exhaust stream or after a concentration step (done by fractionating).

Figure 1: Flowchart of the R134a and SF_6 recovery

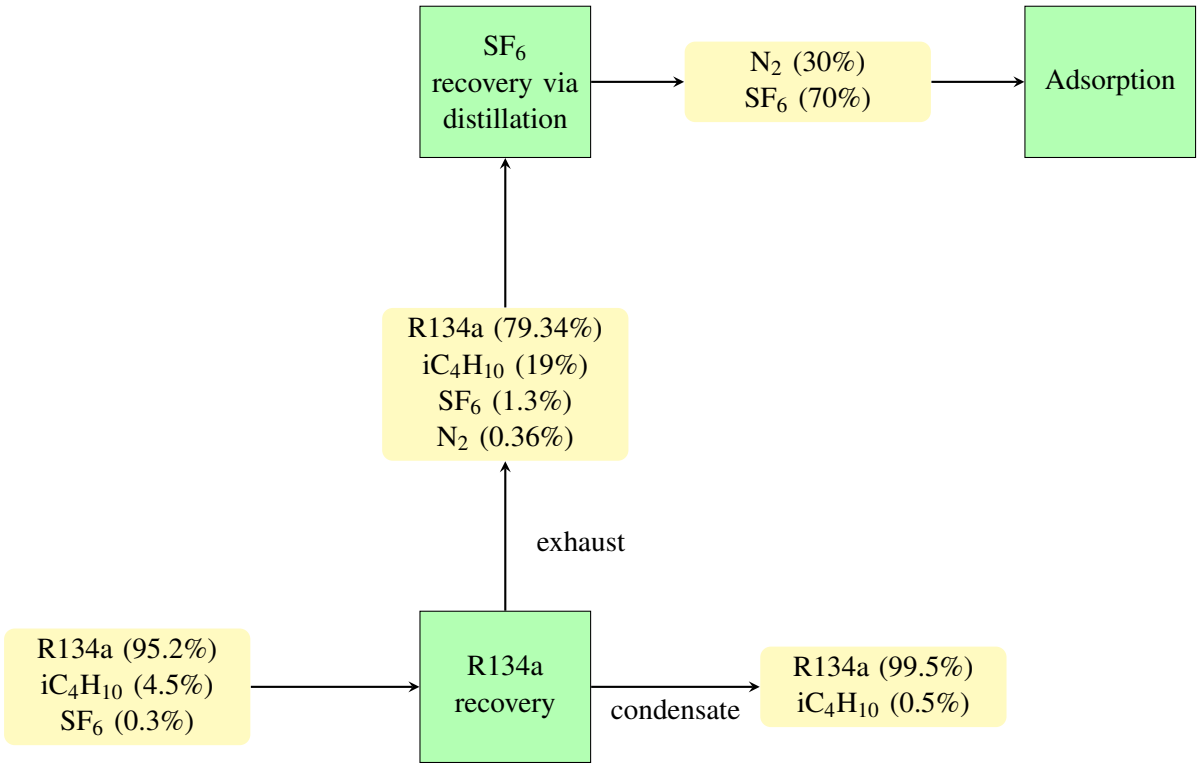

3 Theory

3.1 Gas Separation Techniques

There are several ways to separate gases, which can be broadly categorized into chemical and physical separation technologies. The latter is chosen as we avoid to create by products which may affect the detectors. In the physical-separation family, techniques such as membrane separation, distillation, pressure swing adsorption (PSA), and temperature swing adsorption (TSA) are mostly used.

	Membrane separation	Distillation	Adsorption
Separation Driving force	Interaction forces between membrane material and permeating molecules	Difference in volatility	Gas loading difference

Table 1: Principles of different physical separation methods.

3.2 Pressure Swing Adsorption

Adsorption is a surface phenomenon where a substance (adsorbate) is accumulated on the surface of a solid (adsorbent). The adsorbate can be in a gas or liquid phase. The driving force for adsorption is unsaturated forces at the solid surface which can form bonds with the adsorbate. These forces are typically electrostatic or van der Waals interactions (reversible). The vastly utilized adsorbents include such as silica gel, zeolites, activated carbon, and molecular sieves. PSA is a process that uses pressure differences to selectively adsorb and desorb gases for separation.

The classic two-bed PSA process was patented in the 1960s by Charles Skarstrom, and has come to be known as the Skarstrom cycle. The basic Skarstrom cycle utilizes two identical packed adsorbent beds, which alternate performing the same tasks, as shown in Figure 2. The major steps in the cycle

include: pressurization, adsorption, blowdown, and purge. Moreover, we can add additional pressure equilibration step to save energy. In step 1, feed flows into bed 1, and raises its pressure, while the fully loaded second bed is connected to the extract product. Once the desired pressure has been reached, the system enters step 2, where the more strongly adsorbed component is retained in bed 1 and the gas outlet stream is enriched in the less strongly adsorbed component. A portion of the raffinate product (the inert species exiting as the exhaust during the adsorption) is transferred to the second bed, to help fully regenerate it. Once the first bed has been loaded, and the second bed regenerated, a pressure equalization step may take place.This allows for energy saving by reducing the quantity of gas that needs to be compressed. After the equilibration step, the process repeats, but with the roles of the two beds reversed.

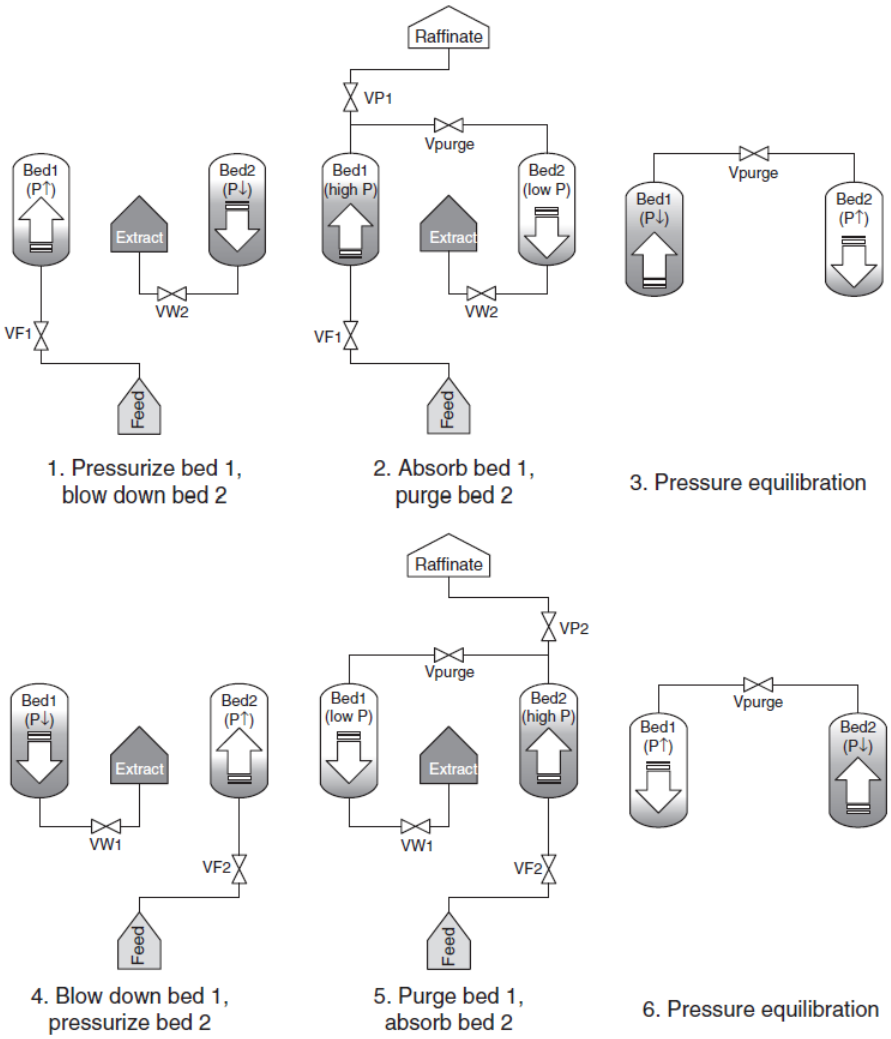

Figure 2: The basic principle of the Skarstrom cycle in the PSA process.

4 Experiment

The goal of the experiment is to determine the potential of PSA process to separate SF_6 from R134a or N_2 and find suitable materials for this purpose. The two materials we tested are zeolite 5A (z5) and 13X (z10). Zeolite 5A is an alkali aluminosilicate carbon available in the form of Type A crystal structure with the pore size 5 Å and 13X is a type of aluminosilicate crystal with a Faujasite structure, characterized by average pores measuring approximately 10 Å [3].

4.1 Experimental Set-up

The four experiments we have conducted are pure R134a and pure SF_6 adsorption in z5 and z10, repectively. Figure 3 shows the experimental set-up of a simplified PSA process.

Figure 3: Experimental set-up of PSA

4.2 Conditions and Procedures

At the beginning of the experiment, we use thermal regeneration (250°C, 1.3 bar with argon as flushing gas) to make sure there's no gas trapped in the material, then start the cycle of the pressure swing adsorption.

Conditions:

- Flowrate: 1-100 L/hr (conversion factor $\sim$ 2.4 air/SF_6) at room temp with gas supply pressure 3 barg (conversion factor = volumetric flow rate of air measured by flowmeter/ volumetric flow rate of specified gas measured by the flowmeter calibrated in air)
- Solid weight: 256g
- Cartridge volume: 0.35 L

Procedures (in cycles):

1. Use a pump to keep the cartridge in medium-high vacuum (-0.92 barg)
2. Feed R134a/SF_6 within the gas cylinder
3. As the pressure of the cartridge increases to 0 barg, stop feeding gas, and restart the cycle

Figure 4 shows the pressure at the input and output of the cartridge and the feed volumetric flowrate during each cycle.

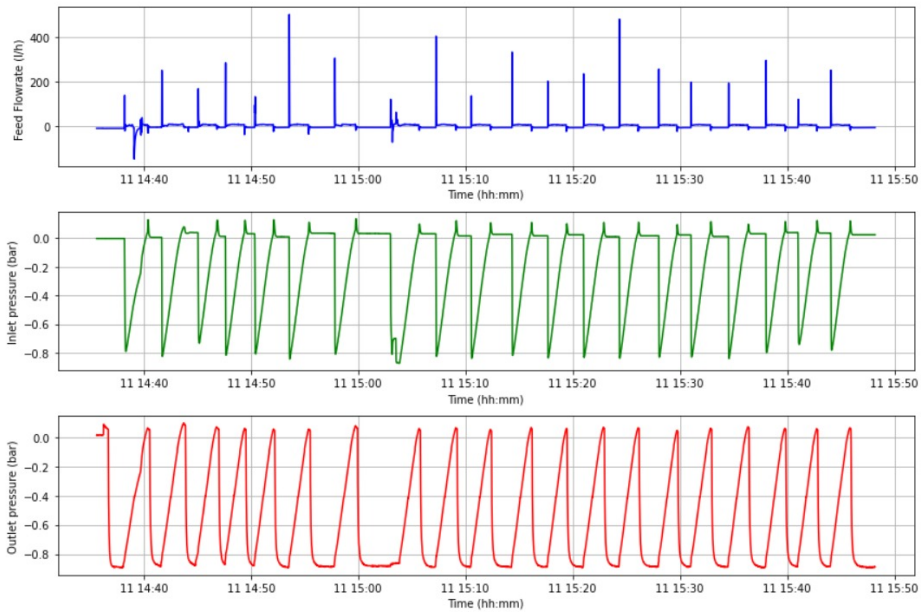

Figure 4: Volumetric flowrate and pressure measured during the experiment

4.3 Result

By the volumetric flowrate measured by the flowmeter, we can calculate the volume of gas inserted into the cartridge in each cycle. Figure 5 shows the converted volume inserted in each cycle, where

$$\text{Converted volume of cycle J} = \frac{1}{\text{conversion factor}} \sum_{i=1}^{t_{\text{end}}} F_i \cdot t_i|_{\text{cycle J}}$$

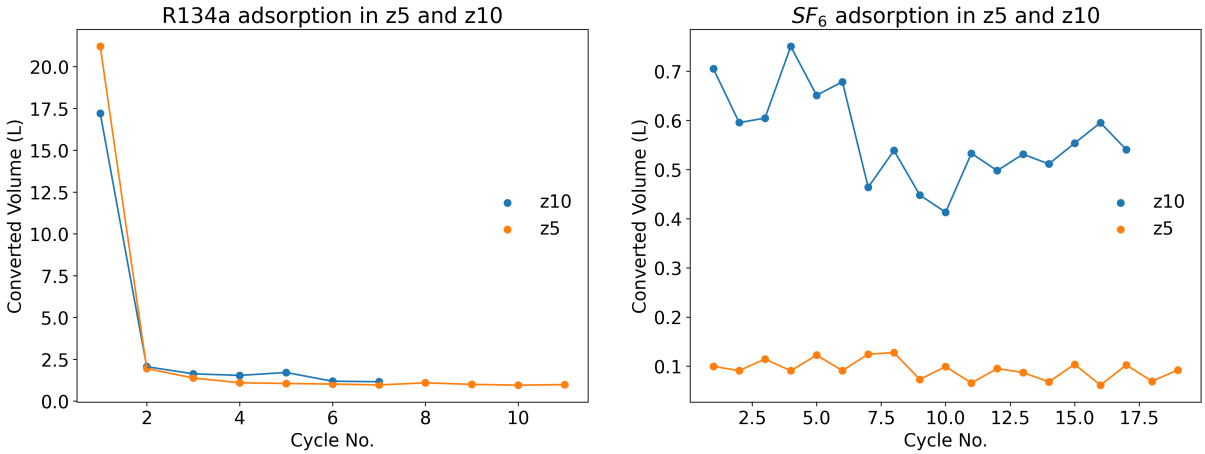

Figure 5: R134a and SF_6 adsorption in z5 and z10

For R134a, the volume inserted drops drastically at the second cycle and reaches a plateau. It may indicate that R134a adsorbed during first cycle is retained in the material even after the pressure regeneration. Therefore, the pressure cycle regeneration may not be enough for R134a, hence thermal regeneration is needed as the desorption requires energy to be supplied to the system. For SF_6, the behavior is very different. First, the volumes inserted within each cycle does not vary significantly, hence pressure cycle regeneration may be sufficient. Secondly, SF_6 adsorbed more in z10 than z5, since

the kinetic diameter of SF_6 (5.5 Å) is larger than the pore size of z5 (5 Å). Lastly, to determine the number of cycles before thermal regeneration for SF_6, more experiments are required.

5 Simulation

The goal of the simulation is to predict the gas-solid interaction and find the input gas pressure and flow rate for the future setups. For this application, we use Aspen Adsorption [4]. Since the data for adsorption isotherm for nitrogen is much easier to obtain, we start the simulation for SF_6/N_2 mixture. The input mixture has a concentration close to the one expected at the output of the SF_6 distillation module.

5.1 Conditions and Parameters

The assumptions of the simulations are:

- Peng-Robingson model was used at equation of state [5]
- In the material balance, the axial dispersion term was neglected (plug flow approximation)
- For the momentum balance, Ergun Equation was used [6]
- The system was considered as non-isothermal with no convection
- A linear lumped resistance to mass transfer was considered (LDF model) [7]
- In terms of geometry, the adsorbent bed is vertical with a single layer containing the z10 adsorbent
- 1D discretization with 20 nodes was considered using the Upwind Differencing Scheme 1 as discretization method

The conditions of the simulations are:

- Volume of the bed: 0.95 m^3
- Temperature: 298.15 K
- Equimolar input: $y_{SF_6,in} = y_{N_2,in} = 0.5$
- Feed flowrate and product flowrate are free variables (depending on ΔP imposed)

For the isotherm parameters, we use Langmuir adsorption model to fit the experimental data from papers [8, 9]:

$$q = q_{max} \frac{bP}{1 + bP}$$

where q [kmol/kg] is the loading, P [bar] is the pressure, b [bar^{-1}] and q_{max} [kmol/kg] are the parameters to be determined. The fitting is done by pyGAPS toolkit and the results are shown in Table 2.

	q_{max} (kmol/kg)	b (bar^{-1})	RMSE
SF_6	2.03 e-3	8.418	0.02957
N_2	1.421e-3	0.2948	0.02362

Table 2: Parameters of SF_6 and N_2 isotherms in z10

5.2 Single Bed Simulation

Before starting a complete PSA simulation, the breakthrough curves were also analyzed. We fixed the input pressure at 3 bar, and analyzed breakthrough curves at three different output pressures.
From Figure 6 we can notice that as pressure difference increases, the output molar fraction of SF_6 reaches a lower value, which favors the separation. Furthermore, we get an idea of breakthrough time in this plot, which would be useful for the setting of PSA cycles.

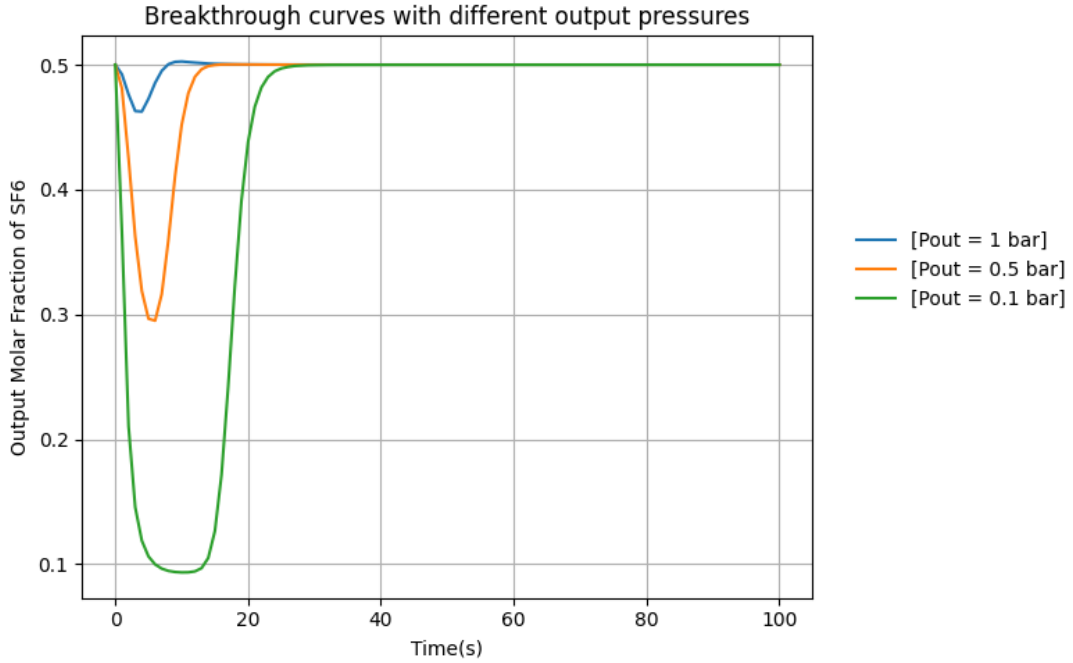

Figure 6: Breakthrough curves ($P_{in} = 3$ bar, $T = 298.15$ K)

5.3 PSA Simulation

5.3.1 Flowsheet

The PSA units operate according to a Skarstrom cycle with four main steps: adsorption, blowdown, purge and pressurization. The complete flowsheet is shown in Figure 7. It is identical to the air separation case study by Wood et al. [10]. For each cycle, the valve specification is stated in Table 3, where 0 means that the valve is fully closed, 1 means fully open, and 2 means that the valve's flow rate has a linear relationship with the pressure drop. The step's duration for step 1 and step 3 are determined by the breakthrough curves, and for step 2 and step 4 are ended till the desired pressure is reached (step 2 ended when $T1a.p \leq P_{out} + 0.1$ and $T2a.p \geq P_{in} - 0.1$, step 4 ended when $T2a.p \leq P_{out} + 0.1$ and $T1a.p \geq P_{in} - 0.1$).

Step	Function	VF1	VF2	VW1	VW2	VP1	VP2	Vpurge
Step1	Adsorb bed 1, purge bed 2	1	0	0	1	1	0	2
Step2	Blowdown bed 1, pressurize bed 2	0	1	1	0	0	1	0
Step3	Purge bed 1, adsorb bed 2	0	1	1	0	0	1	2
Step4	Pressurize bed 1, blowdown bed 2	1	0	0	1	1	0	0

Table 3: Specification of the cycle

Note that for this application, we assume a linear relationship between the pressure drop across

the valve and the flow, we have

$$F = C_v \Delta P$$

The value of C_v used during the simulation is shown in Table 4.

Valve	C_v setting (kmol/(s bar^{-1}))
VF	0.0407
VP	2.78e-5
Vpurge	1.93e-4
VW	0.2784

Table 4: Valve setting

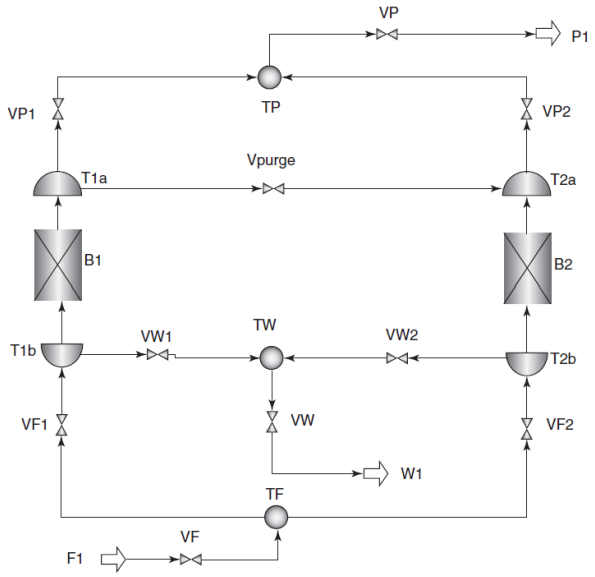

Figure 7: Flowsheet of PSA

5.4 Result

Figure 8 and figure 9 are the PSA results for different output pressure (1 bar and 0.5 bar, respectively), and with an input pressure of 3 bar. In the figure, each color corresponds to different duration time of step 1 and step 3. From figure 6, we know that z10 adsorbs more SF_6 than N_2, hence we expect to have lower molar fraction of SF_6 in the product line. When the output pressure is 1 bar, it decreases at first, but later increases and reaches a plateau. When the output pressure is 0.5 bar, it behaves differently. As a fact, the molar fraction of SF_6 decreases and reaches a plateau.

From figure 9, we can see that as increasing the duration of adsorption phases (step 1 and 3), the purity of the raffinate increases. If we take the first bed as reference, a great portion of its output is used for purging the second bed in order to facilitate regeneration. In fact, as we increase the duration time of step 1, the first bed's output presents a lower quantity of SF_6. Clearly, the reduction of SF_6 in the product line is due to a increase of the beds adsorption capacity. This in turn can be explained by the fact that the longer one bed adsorbs, the longer the other one regenerates, thus making the bed more suitable for adsorption in the next cycles.

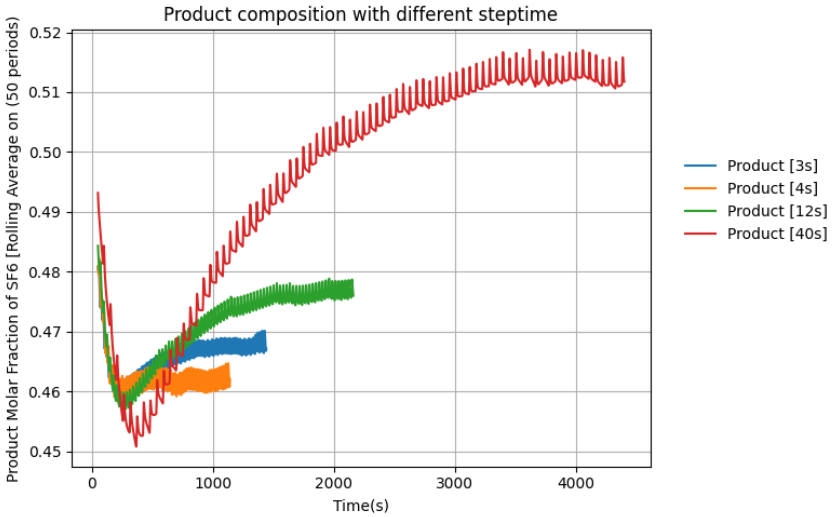

Figure 8: PSA results ($P_{in} = 3$ bar, $P_{out} = 1$ bar)

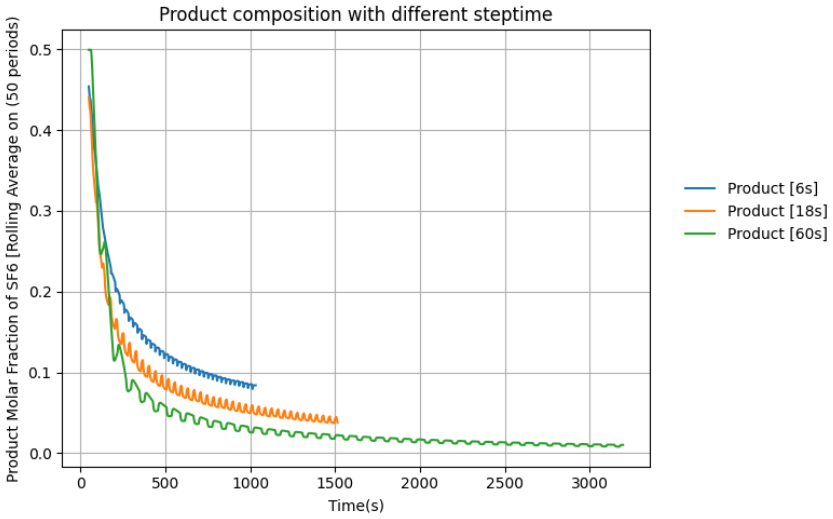

Figure 9: PSA results ($P_{in} = 3$ bar, $P_{out} = 0.5$ bar)

6 Conclusion

To test the possibility using adsorption process for SF_6 recovery, several experiments and simulations were executed. According to the experiments, adsorption in both z5 and z10 are helpful for SF_6 recovery, however, using only pressure swing adsorption may not be feasible since R134a adsorbed strongly in both z5 and z10. Based on the simulation, pressure swing adsorption may be probable for SF_6/N_2 separation, which is helpful at the second stage of SF_6 recovery.

7 Acknowledgements

Special thanks to my supervisors, Damiano Galassi and Maria Cristina Arena, for all their kind help and guidance throughout my summer project. I also want to thank all members of the EP-DT-FS Gas team and the summer student program for their warm support and for making this an unforgettable summer.

Bibliography

[1] Myhre, G., D. Shindell, F.-M. Bréon, W. Collins, J. Fuglestvedt, J. Huang, D. Koch, J.-F. Lamarque, D. Lee, B. Mendoza, T. Nakajima, A. Robock, G. Stephens, T. Takemura and H. Zhang, 2013: Anthropogenic and Natural Radiative Forcing.

[2] CERN, Vol. 3 (2023): CERN Environment Report—Rapport sur l'environnement 2021–2022.

[3] Pérez-Botella, E., Valencia, S., & Rey, F. (2022). Zeolites in adsorption processes: State of the art and future prospects. Chemical Reviews, 122(24), 17647-17695.

[4] Bhatt, T. S., Sliepcevich, A., Storti, G., & Rota, R. (2014). Experimental and modeling analysis of dual-reflux pressure swing adsorption process. Industrial & Engineering Chemistry Research, 53(34), 13448-13458.

[5] Lopez-Echeverry, J. S., Reif-Acherman, S., & Araujo-Lopez, E. (2017). Peng-Robinson equation of state: 40 years through cubics. Fluid Phase Equilibria, 447, 39-71.

[6] Richardson, J.F., Harker, J.H. and Backhurst, J.R. (2002) Coulson and Richardson's Chemical Engineering: Particle Technology and Separation Process, Vol. 2, 5th Edition, Elsevier, New Delhi.

[7] R. B. Bird, W. E. Stewart, E. N. Lightfoot, Transport Phenomena, 2nd Ed., Jone Wiley & Sons, 2002

[8] Wanigarathna, J. A. D. K. (2018). Adsorption-based fluorocarbon separation in zeolites and metal organic frameworks (Doctoral dissertation).

[9] Dunne, J. A., Mariwala, R., Rao, M., Sircar, S., Gorte, R. J., & Myers, A. L. (1996). Calorimetric heats of adsorption and adsorption isotherms. 1. O2, N2, Ar, CO2, CH4, C2H6, and SF6 on silicalite. Langmuir, 12(24), 5888-5895.

[10] Wood, K.R., Liu, Y.A., & Yu, Y. (2018). Design, Simulation and Optimization of Adsorptive and Chromatographic Separations: A Hands-On Approach